Computers and Geotechnics 38 (2011) 577–584

Contents lists available at ScienceDirect

Computers and Geotechnics

journal homepage: www.elsevier.com/locate/compgeo

# Probabilistic infinite slope analysis

D.V. Griffiths [a,1], Jinsong Huang [a,*], Gordon A. Fenton [b,2]

[a] Division of Engineering, Colorado School of Mines, Golden, CO 80401, USA
[b] Department of Engineering Mathematics, Dalhousie University, P.O. Box 1000, Halifax, Nova Scotia, Canada B3J 2X4

ARTICLE INFO

*Article history:*
Received 5 July 2010
Received in revised form 12 January 2011
Accepted 20 March 2011

*Keywords:*
Infinite slope
Stability
Finite element method
Probability of failure
Spatial correlation

ABSTRACT

Research activity in the mechanics of landslides has led to renewed interest in the infinite slope equations, and the need for a more general framework for giving insight into the probability of failure of long slopes involving non-homogeneous vertical soil profiles and variable groundwater conditions. This paper describes a methodology in which parameters such as the soil strength, slope geometry and pore pressures, are generated using random field theory. Within the limitations of the infinite slope assumptions, the paper clearly demonstrates the important "seeking out" effect of failure mechanisms in spatially random materials, and how "first order" methods that may not properly account for spatial variability can lead to unconservative estimates of the probability of slope failure.



## 1. Introduction

Recent interest in the analysis of shallow landslides (e.g. [1–3]) has led to renewed examination of the infinite slope equations as a simple model for assessing the factor of safety of "long" slopes. The infinite slope model is the oldest and simplest slope stability method that assumes identical conditions occur on any vertical section. While the model is not capable of modeling any kind of downslope variability, it is used in this paper to give important insight into the influence of spatial variability on slope failure probability and the location of the critical failure mechanism. The infinite slope equation is usually implemented with the assumption of homogeneous or averaged soil properties in which failure always occurs at the base of the slope. The work described in this paper takes a more general approach, in which one or more of the parameters used in the infinite slope equation are treated as random variables defined by a mean, a standard deviation, and in some cases, a spatial correlation length. Furthermore, in the case of two or more random variables, the analyses described in this paper allow for the option of cross-correlation between parameters. The objective of the analyses is to produce estimates of the probability of infinite slope failure as opposed to the conventional factor of safety.

Consider a typical slice of the infinite slope shown in Fig. 1. The infinite slope equation for the factor of safety ($FS$) of a homogeneous soil in this case (e.g. [4]) is given by

$$FS = \frac{(H\gamma\cos^2\beta - u)\tan\phi' + c'}{H\gamma\sin\beta\cos\beta} \tag{1}$$

where the independent variable names have the following meanings

| | |
|---|---|
| $H$ | depth of the soil layer to the potential failure surface |
| $\beta$ | slope inclination |
| $\gamma$ | total unit weight |
| $u$ | pore pressure at the base of the slice |
| $\phi'$ | effective soil friction angle at the base of the slice |
| $c'$ | effective cohesion at the base of the slice |

In a probabilistic approach to this problem, any of the six input parameters can be defined statistically by a probability density function with a mean and a standard deviation. In the case of parameters such as the shear strength ($c', \tan\phi'$), the unit weight ($\gamma$) and pore pressure ($u$) which are distributed over the depth of the slope, a third parameter, the spatial correlation length which describes the distance over which properties tend to be spatially correlated can be included. Random field (RF) models can account for this parameter, however the paper will start by using some simpler "first order" probabilistic methods. An important finding of this paper will be that methods that do not properly account for the influence of spatial correlation can lead to unconservative reliability estimates.

* Corresponding author. Address: Centre for Geotechnical and Materials Modelling, University of Newcastle, Callaghan, NSW 2308 Australia. Tel.: +61 024921 5118; fax: +61 024921 6946.
*E-mail addresses:* d.v.griffiths@mines.edu (D.V. Griffiths), jinsong.huang@newcastle.edu.au (J. Huang), Gordon.Fenton@dal.ca (G.A. Fenton).
[1] Tel.: +1 (303) 273 3669; fax: +1 (303) 273 3602.
[2] Tel.: +1 (902) 494 6002; fax: +1 (902) 423 1801.

0266-352X/$ - see front matter © 2011 Elsevier Ltd. All rights reserved.
doi:10.1016/j.compgeo.2011.03.006

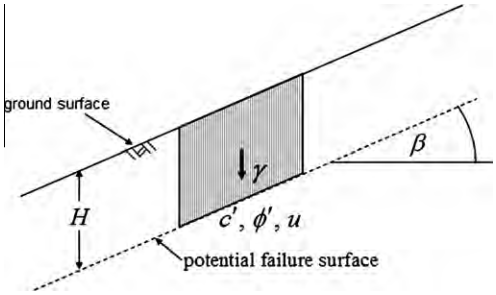


**Fig. 1.** Infinite slope configuration.

In most cases we will assume that random variables (e.g. soil properties, slope angle, pore pressures) are lognormally distributed, which is to say that the log (base $e$) of the variables are normally distributed. The lognormal distribution is one of many possible choices (e.g. [5]) however it offers the advantage of simplicity, in that it is arrived by a simple nonlinear transformation of the classical normal (Gaussian) distribution. Lognormal distributions guarantee that the random variable is always positive, and in addition to the current authors, it has been advocated and used by several other investigators as a reasonable model for physical soil properties (e.g. [6–11]).

## 2. Example 1: undrained clay (random $c_u$)

Although there are six independent variables in Eq. (1), the first infinite slope example considers just one random variable, namely the undrained shear strength $c_u$. Of the other five parameters, two are set to zero ($\tan\phi_u = 0$, $u = 0$) and the other three ($\gamma$, $H$, $\beta$) are set to deterministic constant values. Eq. (1) therefore simplifies to the form

$$FS = \frac{c_u}{\gamma H \sin\beta\cos\beta} \tag{2}$$

The first example problem assumes that the undrained shear strength is defined by $\mu_{c_u} = 25\ \text{kN/m}^2, \sigma_{c_u} = 2.5\ \text{kN/m}^2$, with the other non-zero parameters fixed at $\gamma = 20\ \text{kN/m}^3$, $H = 2.5$ m and $\beta = 30°$. It can be noted that if Eq. (2) is evaluated for this test problem with the undrained shear strength set to the mean value of $\mu_{c_u} = 25\ \text{kN/m}^2$, a factor of safety of $FS = 1.15$ is obtained.

### 2.1. Example 1 by the first order second moment (FOSM) method

Details of this classical method are described elsewhere (e.g. [12,13]). The Factor of Safety given by Eq. (2) is a linear function of a single random variable $c_u$, hence the statistical properties of the dependent variable $FS$ are simply given by

$$\mu_{FS} = \frac{\mu_{c_u}}{\gamma H\cos\beta\sin\beta} = 1.155 \quad \text{and} \quad \sigma_{FS} = \frac{\sigma_{c_u}}{\gamma H\cos\beta\sin\beta} = 0.115 \tag{3}$$

In order to compute the probability of failure, we must assume a distribution for $FS$. Since $c_u$ is lognormal, from Eq. (3) $FS$ will also be lognormal, hence the probability of failure is given by

$$p_f = \text{P}[FS < 1] = \text{P}[\ln(FS) < \ln(1)] = \Phi\left[-\frac{\mu_{\ln FS}}{\sigma_{\ln FS}}\right] \tag{4}$$

where the mean and standard deviation of the underlying normal distribution of $\ln FS$ are given by

$$\sigma_{\ln(FS)} = \sqrt{\ln\{1+v_{FS}^2\}} \quad \text{and} \quad \mu_{\ln(FS)} = \ln\mu_{FS} - \frac{1}{2}\sigma^2_{\ln(FS)} \tag{5}$$

and $v_{FS}$ is the coefficient of variation of FS and $\Phi(\cdot)$ is the cumulative standard normal function.

Using the parameters of the example problem, Eq. (5) give $\mu_{\ln(FS)} = 0.139$ and $\sigma_{\ln(FS)} = 0.100$, which after substitution into Eq. (4) gives

$$p_f = \Phi\left[-\frac{0.13887}{0.09975}\right] = \Phi[-1.39212] = 1 - \Phi[1.39212] = 1 - 0.918 = 0.082 \tag{6}$$

hence the probability of failure is 8.2%.

### 2.2. Example 1 by the first order reliability method (FORM)

A drawback of the FOSM method is that it can lead to non-unique probabilities of failure for the same problem when stated in equivalent, but different ways (e.g. [14–16]). The FOSM method essentially computes the distance from the mean point to the failure surface *in the direction of the gradient at the mean point*. [17] overcame the non-uniqueness issue in the FOSM by looking for the overall minimum distance between the mean point and the failure surface, rather than looking just along the gradient direction. The approach involves optimization, which is easily coded in widely available software such as *Excel* (see e.g. [18,19]).

The Hasofer–Lind implementation is essentially "distribution free" since it makes no assumption about the probability density function of the input random variables. FORM implicitly assumes that the input variables are normally distributed, so if non-normal parameters are required, the user must evaluate "equivalent normal parameters" using the [20] approach or suitable transformations (see also [21,22]). In this paper, only lognormal distributions will be considered, so the equivalency is easily obtained as will be shown.

If $c_u$ is assumed to be lognormal as in the previous example, a simple rearrangement of Eq. (2) leads to

$$FS = \frac{e^{\ln(c_u)}}{\gamma H\sin\beta\cos\beta} \tag{7}$$

in which case $\ln(c_u)$ is normally distributed with $\mu_{\ln(c_u)} = 3.214$ and $\sigma_{\ln(c_u)} = 0.100$ from Eq. (5). A FORM analysis[3] operating on Eq. (7) leads to $p_f = 0.082$ (8.2%) in exact agreement with FOSM which is to be expected in this case for a linear function of a single normal random variable (e.g. [23]).

### 2.3. Example 1 by the random field method

In this section we present results obtained using a random field model of the infinite slope. In this case a typical column from the slope is split into 100 equal slices and a 1-d random field of the required property assigned to each slice as shown in Fig. 2. The choice of 100 slices was considered a reasonable compromise after performing parametric studies going up to 10,000. As a general rule, the greater the number of slices, the higher the computed probability of failure, but the difference was only significant at the lowest spatial correlation lengths. The methodology for generating random fields has been described in detail elsewhere, so the interested reader is referred to other publications (e.g. [5]).

In addition to the mean and standard deviation of the property being considered, this approach allows the inclusion of an additional parameter called the spatial correlation length $\theta$, also known as the scale of fluctuation. Loosely speaking, $\theta$ is a dimensional property representing the distance within which properties are significantly correlated (or the log of the property if the field is assumed lognormal). Conversely, properties separated by a distance

[3] The FORM programs used for the three examples described in this paper are all available from the first author's web site at http://inside.mines.edu/~vgriffit/FORM/Infinite_Slope_Paper.

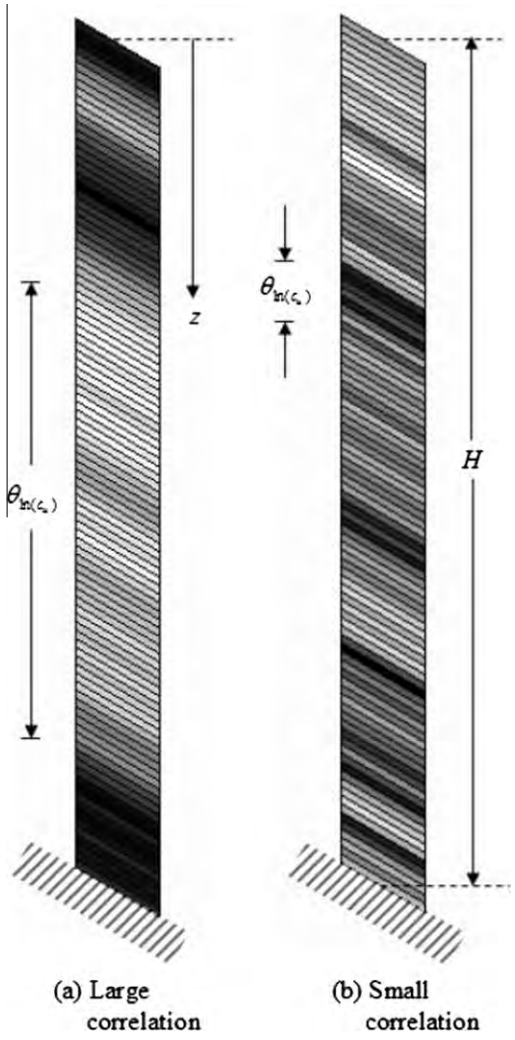


**Fig. 2.** Typical random fields of $c_u$ with (a) large spatial correlation and (b) small spatial correlation.

of more than $\theta$ are largely uncorrelated. Mathematically, $\theta$ is defined here as the area under the correlation function [24]. Fig. 2 shows a grayscale which portrays a random field of a soil property (e.g. $\ln(c_u)$) in which black implies high values and white implies low. A large spatial correlation length indicates that the soil property is varying slowly (Fig. 2a) while a small value indicates that it is varying rapidly (Fig. 2b) A key factor however, is that while the fields look quite different from each other, they have the same mean and standard deviation of the property being modeled on average.

After the random field has been generated and assigned to the slices, the factor of safety of each slice is computed using Eq. (2). It should be noted that when implementing Eq. (1), $H$ is replaced by the depth $z$ of each slice (see also Eq. (10)). In the case where the soil column is modeled by 100 slices, the approach leads to 100 different factors of safety of which the smallest is recorded as the "correct" value for that particular simulation. It may be noted that a homogeneous slope ($c_u$ = constant) analyzed this way would also lead to 100 different factors of safety, however in this case the factor of safety would monotonically decrease with depth, and the minimum value would always occur at the base of the soil column ($z = H$) where $z$ is a maximum. In the random field case however, the lowest factor of safety of the set does not necessarily occur at the base.

The random field approach then performs Monte-Carlo simulations, which means that the analysis just described is repeated many times. Each repetition of the analysis involves the generation of a random field with the same mean and standard deviation, but with a different spatial distribution of properties each time. For example in one simulation, the strong soil elements may be near the bottom of the column, whereas on another they may be near the top.

All results presented in this section used 5000 Monte-Carlo simulations, which were found to give satisfactory statistical reproducibility. Further discussion of the influence of the number of simulations on the standard error of the output mean and standard deviation can be found in [25]. Following each simulation, the minimum factor of safety $FS$ and the critical depth at which it occurred were recorded. From the resulting 5000 $FS$ values, the probability of failure was computed simply as the proportion of those 5000 results in which $FS < 1$.

Fig. 3 shows the computed probability of failure for the test problem assuming a lognormally distributed $c_u$ over a range of spatial correlation lengths $\Theta$, defined in dimensionless form as

$$\Theta = \frac{\theta_{\ln(c_u)}}{H} \tag{8}$$

where $\theta_{\ln(c_u)}$ is the actual correlation length in meters. A Markov correlation function has been used in this paper of the form

$$\rho = e^{-2\tau/\theta_{\ln(c_u)}} \tag{9}$$

where $\rho$ is the correlation coefficient and $\tau$ is the vertical distance between points. In view of the lack of evidence supporting any particular form of correlation function (e.g. [26]), the Markov function has been used on the grounds of its simplicity in which only one parameter needs to be computed.

The result clearly demonstrates the unconservative nature of the first order approaches. The random field solutions give a higher probability of failure for all reasonable correlation lengths and only converge asymptotically on the first order solution as the correlation length becomes very large ($\Theta \to \infty$). This convergence emphasizes the fact that first order approaches are "single random variable" methods in which the soil column is always assumed to be homogeneous, albeit with a shear strength that can vary randomly.

## 3. Further observations on the random field results

### 3.1. Location of the critical failure plane

Consider once more Eq. (2) with the column depth $H$ replaced by the depth coordinate $z$ to give

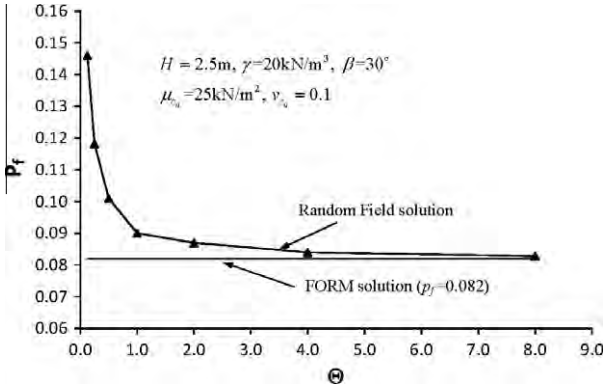


**Fig. 3.** Comparison of FORM and random field results for the undrained clay Example 1 ($\phi_u = 0$) showing the influence of the spatial correlation length $\Theta$.

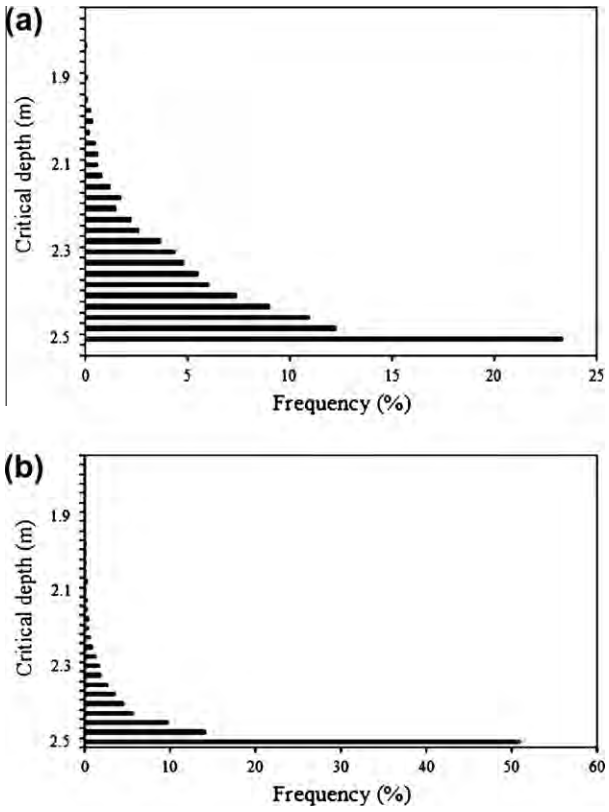


**Fig. 4.** Histograms showing the frequency of the critical depth from the random field analyses of Example 1. (a) $\Theta = 0.04$, (b) $\Theta = 1.28$.

$$FS = \frac{c_u}{\gamma z \sin\beta \cos\beta} \tag{10}$$

The minimum factor of safety will occur where $c_u/z$ is at a minimum (e.g. [27]). When $c_u$ is treated as a spatially random variable however, the minimum value of $c_u/z$, and hence the critical failure surface, will not necessarily occur at the base of the column. Fig. 4a and b show histograms of the frequency with which the critical failure plane occurred at different depths for two different spatial correlation lengths. Both histograms indicate that a significant proportion of critical failure planes occur above the base. The histogram shown in Fig. 4a for $\Theta = 0.04$, indicates that only about 23% of the critical mechanisms occurred at the base with 77% occurring higher up the soil column. This is because with small correlation lengths, there is a greater probability of the minimum $c_u/z$ occurring higher up the column, even though $z$ is also smaller at higher elevations. For the higher spatial correlation length of $\Theta = 1.28$ shown in Fig. 4b, the percentage of mechanisms occurring at the base ($\approx$51%) is considerably increased as the random field becomes more spatially uniform, where it is less likely that the minimum $c_u/z$ will occur at higher elevations.

### 3.2. Finite element deformation analyses

The above example involved substitution of parameters into the infinite slope equations and involved no concept of deformation. In order to emphasize the varying locations of the critical failure plane, an additional set of analyses have been performed using the random elasto-plastic finite element method (RFEM) (e.g. [28–31]). These analyses have the ability to indicate failure deformations as well as factors of safety corresponding to each Monte-Carlo simulation. Fig. 5 shows some deformed meshes for simulations that were deliberately chosen because they gave

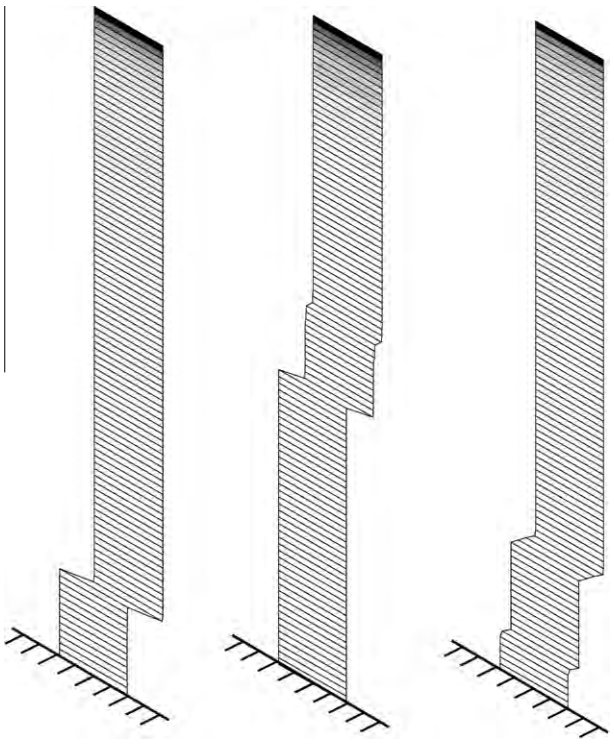

**Fig. 5.** Typical failure modes from RFEM analyses with $v_{c_u} = 0.1$ and $\Theta = 0.25$ showing mechanisms well removed from the base of the column (grayscale shows relative values of $c_u/z$).

mechanisms that were well removed from the base. It is interesting to observe that some simulations display more than one failure mechanism, implying more than one location exhibiting the same (minimum) factor of safety and failing at the same time.

### 3.3. Distribution of FS values

In the previous sub-section, the probability of failure $p_f$ was computed simply as the proportion of the total number of Monte-Carlo simulations that resulted in $FS < 1$. Since each random field simulation computes a different minimum factor of safety, the full probability density function of $FS$ values can be plotted and used for further analysis. Fig. 6 shows the lognormal probability density functions of the input undrained strength $c_u$ for two different coefficients of variation given by $v_{c_u} = 0.1$ and $v_{c_u} = 0.5$. Both cases have the same mean of $\mu_{c_u} = 25$ kN/m$^2$ and spatial

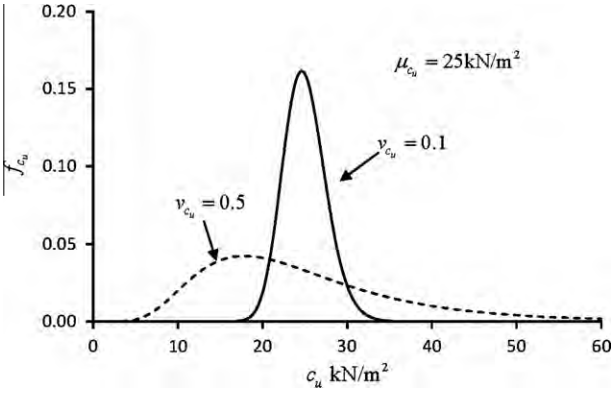


**Fig. 6.** Distributions of input undrained strength corresponding to low ($v_{c_u} = 0.1$) and high ($v_{c_u} = 0.5$) input coefficients of variation.

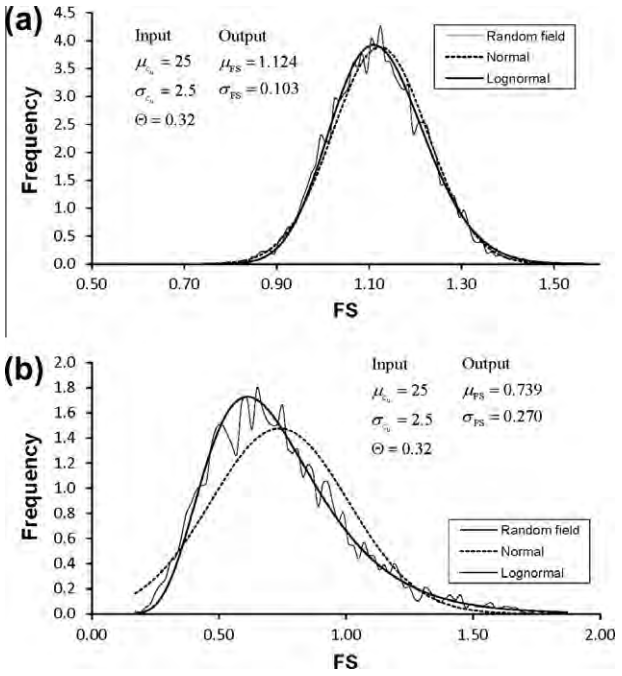


**Fig. 7.** Histogram of *FS* frequency distribution for Example 1 together with normal and lognormal fits based on the computed mean and standard deviation. (a) $v_{c_u} = 0.1$, (b) $v_{c_u} = 0.5$.

correlation length of $\Theta = 0.32$. Fig. 7a and b show the computed probability density plots of *FS* values for both cases. Also included on the figures are analytical normal and lognormal fits to the factor of safety distributions based on the computed mean and standard deviation values. In Fig. 7a for the lower input coefficient of variation, both analytical curves agree well with the random field results as might be expected in view of the low input variation.

Fig. 7b shows similar fits for the higher input coefficient of variation indicating that the slope now has a very high probability of failure. The figure also illustrates that for higher input variability, the distribution of *FS* is much better fitted to the lognormal distribution, which might be expected considering that the input random variable on the right hand side of Eq. (3) is also lognormal. Although this aspect will not be pursued here, lognormal distributions such as those illustrated in Fig. 7a and b could also be used to make estimates of the probability of the factor of safety falling below some "design value".

It can also be noted, that with a low input coefficient of variation of $v_{c_u} = 0.1$ as shown in Fig. 7a, the computed mean and standard deviation of the factor of safety as ($\mu_{FS} = 1.124$ and $\sigma_{FS} = 0.103)_{\text{Random}}$ are quite close to those obtained by the first order method from Eq. (5), namely ($\mu_{FS} = 1.155$ and $\sigma_{FS} = 0.115)_{\text{1stOrder}}$. For the case with a higher coefficient of variation of $v_{c_u} = 0.5$ as shown in Fig. 7b however, the results given as ($\mu_{FS} = 0.739$ and $\sigma_{FS} = 0.270)_{\text{Random}}$ and ($\mu_{FS} = 1.155$, $\sigma_{FS} = 0.578)_{\text{1stOrder}}$ respectively are quite different, confirming that first order assumptions are only justified for low input coefficient of variation.

## 4. Example 2: frictional/cohesive soil (random $c'$ and tan $\phi'$)

We now consider an effective stress analysis of the infinite slope problem with shear strength parameters given by $c'$ and tan $\phi'$ with no pore pressures included. In this case Eq. (1) simplifies to

$$FS = \frac{c'}{\gamma H \sin\beta\cos\beta} + \frac{\tan\phi'}{\tan\beta} \tag{11}$$

Here we consider random $c'$ and tan $\phi'$. The parameter tan $\phi'$ will be modeled as a random variable (rather than $\phi'$ itself) in view of the fundamental nature of tan $\phi'$ in the Coulomb strength equation. A lognormal distribution of tan $\phi'$ will ensure the friction angle is bounded by $0 < \phi' < 90°$. While it is recognized that very high friction angles will occasionally be generated, it is felt that the lognormal distribution represents a reasonable compromise at the point level, where small pockets of very strong material may be encountered. Some investigators have advocate a bounded distribution for the frictional strength such as the "tanh-distribution" (see e.g. [5]) however demonstrations of this distribution is left for future studies.

This second example problem gives both shear strength parameters a coefficient of variation $v_{c',\tan\phi'} = 0.3$ in which the cohesion is defined by $\mu_{c'} = 10$ kN/m$^2$ and $\sigma_{c'} = 3.0$ kN/m$^2$ and the tangent of the friction angle by $\mu_{\tan\phi'} = 0.5774$ and $\sigma_{\tan\phi'} = 0.1732$ (corresponding to $\mu_{\phi'} \approx 30^\circ$ and $\sigma_{\phi'} \approx \sigma_{\tan\phi'}\cos\mu_{\phi'} = 8.6^\circ$ to a first order of accuracy). The random variables are assumed to be uncorrelated and lognormal. The remaining parameters from Eq. (11) in this example are assumed to be deterministic with values given by $H = 5.0$ m, $\beta = 30°$, $\gamma = 17.0$ kN/m$^3$ and $u = 0$. Substitution of these deterministic parameters and the mean values of the random variables into Eq. (11) lead to a deterministic factor of safety of $FS = 1.27$.

### 4.1. Example 2 by the first order second moment method (FOSM)

From Eq. (11), and assuming $c'$ and tan $\phi'$ are uncorrelated, we can estimate the mean and standard deviation of *FS* by the FOSM as

$$\mu_{FS} \approx \frac{\mu_{c'}}{\gamma H \sin\beta\cos\beta} + \frac{\mu_{\tan\phi'}}{\tan\beta} \tag{12}$$

and

$$\sigma_{FS} \approx \sqrt{\left(\frac{1}{\gamma H \sin\beta\cos\beta}\right)^2 \sigma_{c'}^2 + \left(\frac{1}{\tan\beta}\right)^2 \sigma_{\tan\phi'}^2} \tag{13}$$

which gives $\mu_{FS} = 1.27$ and $\sigma_{FS} = 0.311$

Assuming that *FS* is lognormal, the probability of failure is then given by

$$p_f = \mathrm{P}[FS < 1] = \mathrm{P}[\ln(FS) < \ln(1)] = \Phi\left[-\frac{\mu_{\ln FS}}{\sigma_{\ln FS}}\right] \tag{14}$$

where the mean and standard deviation of the underlying normal distribution of ln (*FS*) from Eq. (5) are given by $\mu_{\ln(FS)} = 0.2113$ and $\sigma_{\ln(FS)} = 0.2409$. After substitution into Eq. (14)

$$p_f = \Phi\left[-\frac{0.2113}{0.2409}\right] = \Phi[-0.8772] = 1 - \Phi[0.8772]$$
$$= 1 - 0.810 = 0.190 \tag{15}$$

hence the probability of failure is 19.0%.

### 4.2. Example 2 by the first order reliability method (FORM)

If $c'$ and tan $\phi'$ are assumed to be lognormal, a simple rearrangement of Eq. (10) leads to

$$FS = \frac{e^{\ln(c')}}{H\gamma \sin\beta\cos\beta} + \frac{e^{\ln(\tan\phi')}}{\tan\beta} \tag{16}$$

In which case ln ($c'$) and ln(tan $\phi'$) are normally distributed with $\mu_{\ln(c')} = 2.259$, $\sigma_{\ln(c')} = 0.294$ and $\mu_{\ln(\tan\phi')} = -0.592$, $\sigma_{\ln(\tan\phi')} = 0.294$ from Eq. (5).

For comparison with the FOSM result of the previous section, when no correlation was assumed between $c'$ and tan $\phi'$, FORM

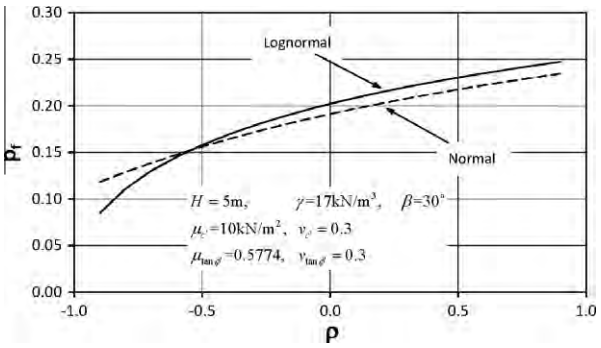


**Fig. 8.** Influence of the correlation coefficient $\rho$ (between $c'$ and $\tan\phi'$) on the probability of failure $p_f$ by FORM.

gave $p_f = 0.202$ (20.2%) which is in close agreement with the FOSM result presented in the previous section.

*4.2.1. Influence of cross-correlation*

The results of an investigation by FORM into the influence of the correlation coefficient acting between $\ln(c')$ and $\ln(\tan\phi')$ is shown in Fig. 8. For comparison, the results obtained with normally distributed $c'$ and $\tan\phi'$ have also been included in the figure as a dotted line. It can be noted that the lognormal and normal responses are quite similar given the relatively low variability of the random input parameters. The probability of failure $p_f$ appears quite sensitive to the correlation coefficient $\rho$ however, and for the lognormal case varies in the range $0.085 \leqslant p_f \leqslant 0.247$, with the highest probability of failure corresponding to the highest positive correlation between $c'$ and $\tan\phi'$. This trend is to be expected (e.g. [32]) since with positive correlation $c'$ and $\tan\phi'$ are both either small, or large at the same time, resulting in a relatively greater probability of failure.

*4.3. Example 2 by the random field method*

The random field model has also been applied to the $c' - \tan\phi'$ slope with the same parametric variations considered in the previous section. In addition, a range of spatial correlation lengths was defined in dimensionless form as

$$\Theta = \frac{\theta_{\ln(c')}}{H} = \frac{\theta_{\ln(\tan\phi')}}{H} \tag{17}$$

The results shown in Fig. 9 indicate a similar trend to that observed previously in Example 1 for the undrained clay, namely that the FORM results are unconservative in underestimating the probability of failure for all but the longest spatial correlation lengths. It

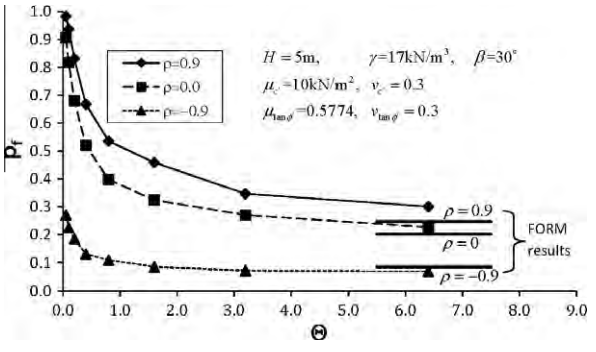


**Fig. 9.** Comparison of FORM and Random Field results for the $c' - \tan\phi'$ Example 2 showing the influence of the spatial correlation length $\Theta$ and correlation.

may also be noted that the random field results exhibited the same trend as FORM in relation to the cross-correlation between strength parameters, with greater positive correlation leading to higher probabilities of failure (e.g. [33]).

## 5. Example 3: frictional soil with pore pressures (random tan $\phi'$, tan $\beta$, $\gamma$ and $u$)

This example is similar to the infinite slope case considered by [34], and involves a cohesionless soil layer containing a random pore pressure. In this study we will assume steady seepage parallel to the ground surface leading to a pore pressure that decreases linearly above the base according to

$$u_z = \begin{cases} 0 & \text{if } H - z \geqslant u/(\gamma_w \cos^2\beta) \\ u - (H-z)\gamma_w \cos^2\beta & \text{if } H - z < u/(\gamma_w \cos^2\beta) \end{cases} \tag{18}$$

where $0 \leqslant z \leqslant H$ is the depth below the ground surface, $u$ is the pore pressure at the base of the column when $z = H$ and $0 \leqslant u_z \leqslant u$ is the pore pressure at depth $z$.

In this case, four out of the six parameters, namely tan $\phi'$, tan $\beta$, $\gamma$ and $u$ from Eq. (1) are assumed to be random, with the properties given in Table 1.

The remaining two parameters are deterministic with values fixed at $c' = 0$ and $H = 5$ m. In this case, Eq. (1) simplifies to

$$FS = \frac{\tan\phi'}{\tan\beta}\left(1 - \frac{u(1+\tan^2\beta)}{\gamma H}\right) \tag{19}$$

where $u$ is given by Eq. (18). Note that the input values $\mu_{\tan\beta} = 0.325$ and $\sigma_{\tan\beta} = 0.033$ from Table 1 imply that to a first order of accuracy $\mu_\beta \approx 18°$ and $\sigma_\beta \approx 1.9°$. Furthermore, when the mean values from Table 1 are substituted into Eq. (19), the deterministic factor of safety is $FS = 1.514$. It may be commented that the lognormal distribution for random variable tan $\beta$ may not be the best choice, however our goal in this example was to compare our results with results of other investigators who had made this assumption.

*5.1. Example 3 by the first order second moment method (FOSM)*

From Eq. (19), and assuming tan $\phi'$, tan $\beta$, $\gamma$ and $u$ are uncorrelated, we can estimate the mean and standard deviation of $FS$ by the FOSM as

$$\mu_{FS} \approx \frac{\mu_{\tan\phi'}}{\mu_{\tan\beta}}\left(1 - \frac{\mu_u(1+\mu^2_{\tan\beta})}{\mu_\gamma H}\right) \tag{20}$$

and

$$\sigma_{FS} \approx \sqrt{\left(\frac{\partial(FS)}{\partial(\tan\phi')}\right)^2 \sigma^2_{\tan\phi'} + \left(\frac{\partial(FS)}{\partial(\tan\beta)}\right)^2 \sigma^2_{\tan\beta} + \left(\frac{\partial(FS)}{\partial\gamma}\right)^2 \sigma^2_\gamma + \left(\frac{\partial(FS)}{\partial u}\right)^2 \sigma^2_u} \tag{21}$$

where the closed-form derivative terms are given in the Appendix A. Evaluation of Eqs. (20) and (21) using mean values gives $\mu_{FS} = 1.514$ and $\sigma_{FS} = 0.481$.

Assuming that $FS$ is lognormal, the probability of failure is then given by

**Table 1**
Input values of for Example 3.

| Variable | Distribution | Mean | SD |
|---|---|---|---|
| tan $\beta$ | Lognormal | 0.325 | 0.0325 |
| tan $\phi'$ | Lognormal | 0.577 | 0.1732 |
| $\gamma$ | Lognormal | 18.000 | 0.5 |
| $u$ | Lognormal | 12.0 | 1.2 |

$$p_f = \mathrm{P}[FS < 1] = \mathrm{P}[\ln(FS) < \ln(1)] = \Phi\left[-\frac{\mu_{\ln FS}}{\sigma_{\ln FS}}\right] \quad (22)$$

where the mean and standard deviation of the underlying normal distribution of ln (*FS*) from Eq. (5) are given by $\mu_{\ln(FS)} = 0.366$ and $\sigma_{\ln(FS)} = 0.310$. After substitution into Eq. (22)

$$p_f = \Phi\left[-\frac{0.366}{0.310}\right] = 0.119 \quad (23)$$

hence the probability of failure is 11.9%.

### 5.2. Example 3 by the first order reliability method (FORM)

If all four random variables are assumed to be lognormal, a rearrangement of Eq. (19) leads to

$$FS = \frac{e^{\ln(\tan\phi')}}{e^{\ln(\tan\beta)}}\left(1 - \frac{e^{\ln(u)}(1 + e^{2\ln(\tan\beta)})}{e^{\ln(\gamma)}H}\right) \quad (24)$$

With no cross-correlations between the random variables, FORM gives a probability of failure of $p_f = 0.113$ (11.3%) which is in close agreement with the FOSM result presented in the previous section.

### 5.3. Example 3 by the random field method

Unlike the first two examples, this case includes random variables of different types. The slope angle tan $\beta$ and the pore pressure at the base $u$ are single random variables that do not involve a spatial correlation, length while the variables tan $\phi'$ and $\gamma$ are typical random field variables, which are spatially distributed along the soil column with the same correlation length $\Theta$ as shown in Fig. 2.

The results of the random field analyses for a range of correlation lengths are shown in Fig. 10. As in the previous examples, the FORM result is shown to be unconservative and a special case of the random field results as $\Theta \to \infty$.

Fig. 11a and b show the frequency with which the critical failure plane occurs at different depths for two different spatial correlation lengths. The mean water surface is at a depth of about 3.65 m below ground surface, and due to these pore pressures, both the low and high spatial correlation length cases indicate that the critical depth is most likely to occur at the bottom of the column. Since the soil under consideration in this example is cohesionless, the histogram shown in Fig. 11a for a low spatial correlation length ($\Theta = 0.05$) displays a rather uniform frequency above the mean water table, indicating that the critical depth has no preferential location in this region. For a higher spatial correlation length ($\Theta = 2.0$) however, the factor of safety is also changing gradually and is either increasing or decreasing with depth. This explains the "bimodal" appearance of the histogram shown in Fig. 11b, where the critical depth is most likely, on average, to occur either at the top or the bottom of the soil column.

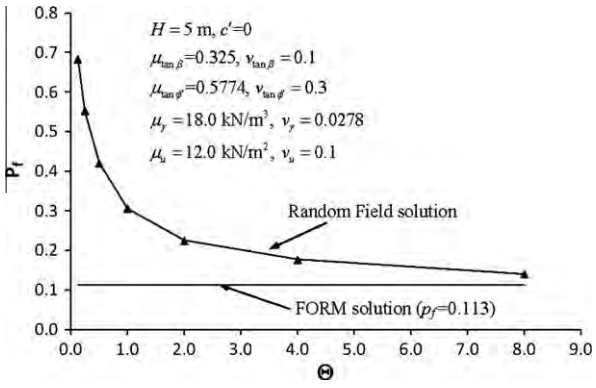


**Fig. 10.** Comparison of FORM and Random Field results for Example 3 showing the influence of the spatial correlation length $\Theta$ (lognormally distributed tan $\phi'$).

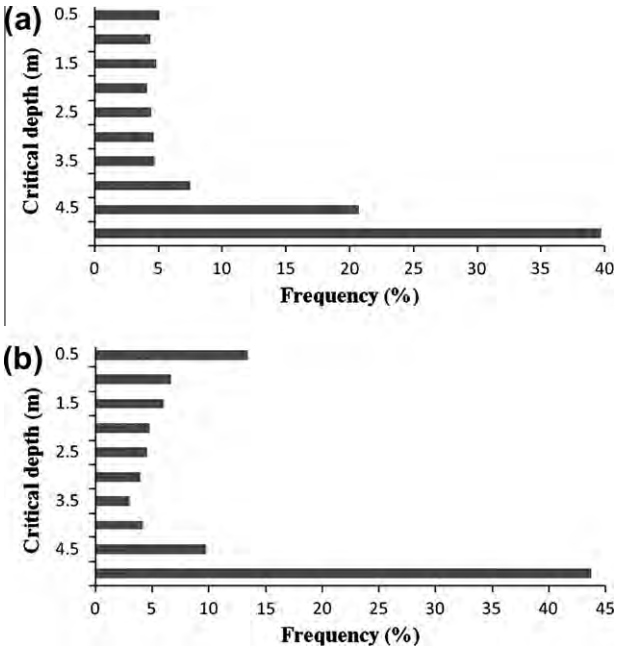


**Fig. 11.** Histograms showing the frequency of the critical depth from the random field analyses of Example 3. (a) $\Theta = 0.05$, (b) $\Theta = 2.0$.

## 6. Concluding remarks

Probabilistic slope stability methods that predefine the potential failure surface using deterministic methods are liable to overestimate the factor of safety or underestimate the probability of failure. This is because they do not allow the failure surface to "seek out" the most critical path through the soil. While this conclusion is also valid for 2D and 3D slope geometries, the infinite slope model offers a particularly striking example of this effect, since the system exhibits no progressive failure and is essentially "brittle", whereby the first component to fail results in overall system failure. First order methods (e.g. FOSM and FORM) applied to the infinite slope problem gave very similar results to each other, but inevitably underestimated the probability of failure compared with the random field analyses, because the failure plane in those cases is always assumed to occur at the base of the soil column. The random field analyses showed that there is a significant probability that the critical mechanism will occur above the base of the soil column where the factor of safety is lower. While the random field analyses predicted higher probabilities of failure than the first order methods, it was observed that the random field results converged on the first order values as the spatial correlation length was increased. This is to be expected, because as the spatial correlation length increases, the greater homogeneity of the soil column means that the probability of the critical mechanism occurring above the base is reduced.

## Acknowledgements

The authors wish to acknowledge the support of NSF Grants CMS-0408150 on "Advanced probabilistic analysis of stability problems in geotechnical engineering", CMMI-0970122 on "GOALI: Probabilistic Geomechanical Analysis in the Exploitation of Unconventional Resources" and KGHM Cuprum, Wroclaw, Poland

through the Framework 7 EU project on "Industrial Risk Reduction" (IRIS).

## Appendix A

Derivative terms used in Example 3

$$\frac{\partial(FS)}{\partial(\tan\phi')} = \frac{1}{\tan\beta}\left(1 - \frac{u(1+\tan^2\beta)}{\gamma H}\right)$$

$$\frac{\partial(FS)}{\partial(\tan\beta)} = -\frac{\tan\phi'}{\tan^2\beta}\left(1 - \frac{u(1+\tan^2\beta)}{\gamma H}\right) - \frac{2u\tan\phi'}{\gamma H}$$

$$\frac{\partial(FS)}{\partial\gamma} = \frac{(1+\tan^2\beta)}{\tan\beta}\frac{u\tan\phi'}{\gamma^2 H}$$

$$\frac{\partial(FS)}{\partial u} = -\frac{(1+\tan^2\beta)}{\tan\beta}\frac{\tan\phi'}{\gamma H}$$

## References

[1] Turner AK, Schuster RL. Proceedings of the 1st North American landslide conference, landslides and society, Pub. Assoc. Environ. Eng. Geol. p. 261–76.
[2] Silva F, Lambe TW, Marr WA. Probability and risk of slope failure. J Geotech Geoenviron Eng 2008;134(12):1691–9.
[3] Zolfaghari A, Heath AC. A GIS application for assessing landslide hazard over a large area. Comput Geotech 2008;35(2):278–85.
[4] Biondi G, Cascone E, Magueri M, Motta E. Seismic response of saturated cohesionless slopes. Soil Dynam Earthquake Eng 2000;20(1–4):209–15.
[5] Fenton GA, Griffiths DV. Risk assessment in geotechnical engineering. John Wiley & Sons: Hoboken, N.J.; 2008.
[6] Parkin TB, Meisinger JJ, Chester ST, Starr JL, Robinson JA. Evaluation of statistical estimation methods for lognormally distributed variables. Soil Sci Soc Am J 1988;52(2):323–9.
[7] Parkin TB, Robinson JA. Analysis of lognormal data. Adv Soil Sci 1992;20:193–235.
[8] Brejda JJ, Moorman TB, Smith JL, Karlen DL, Allan DL, Dao TH. Distribution and variability of surface soil properties at a regional scale. Soil Sci Soc Am J 2000;64(3):974–82.
[9] Gui SX, Zhang RD, Turner JP, Xue XZ. Probabilistic slope stability analysis with stochastic soil hydraulic conductivity. J Geotech Geoenviron Eng 2000;126(1):1–9.
[10] Nour A, Slimani A, Laouami N. Foundation settlement statistics via finite element analysis. Comput Geotech 2002;29(8):641–72.
[11] Massih DSYA, Soubra AH, Low BK. Reliability-based analysis and design of strip footings against bearing capacity failure. J Geotech Geoenviron Eng 2008;134(7):917–28.
[12] Harr ME. Reliability-based design in civil engineering. New York: McGraw-Hill; 1987.
[13] Baecher GB, Christian JT. Reliability and statistics in geotechnical engineering. Hoboken, NJ: J. Wiley; 2003.
[14] Ditlevsen, Structural reliability and the invariance problem, Research Report No. 22. Solid mechanics division. Waterloo, Canada: University of Waterloo; 1973.
[15] Madsen HO, Krenk S, Lind NC. Methods of structural safety. Englewood Cliffs, NJ: Prentice-Hall; 1985.
[16] Nadim F, Einstein H, Roberds W. Probabilistic stability analysis for individual slopes in soil and rock, State-of-the-Art Paper 3. International Conference on Landslide Risk Management. 2005. Vancouver, Canada.
[17] Hasofer AM, Lind NC. Exact and invariant second-moment code format. J Eng Mech Div-Asce 1974;100:111–21.
[18] Low BK, Tang WH. Efficient reliability evaluation using spreadsheet. J Eng Mech-Asce 1997;123(7):749–52.
[19] Low BK. Practical probabilistic slope stability analysis. In Proceedings, soil and rock America 2003, 12th Panamerican conference on soil mechanics and geotechnical engineering and 39th U.S. rock mechanics symposium. MIT. Cambridge, Massachusetts: Verlag Glückauf GmbH Essen; 2003. p. 2777–84.
[20] Rackwitz R, Flessler B. Structural reliability under combined random load sequences. Comput Struct 1978;9(5):489–94.
[21] Hohenbichler M, Rackwitz R. Non-normal dependent vectors in structural safety. J Eng Mech Div-Asce 1981;107(6):1227–38.
[22] Hohenbichler M, Gollwitzer S, Kruse W, Rackwitz R. New light on first- and second-order reliability methods. Struct Safety 1987;4(4):267–84.
[23] Schiermeyer RL. Probabilistic methods applied to slopes and footings. Masters Thesis. Division of Engineering, Colorado School of Mines: Golden, CO; 2009.
[24] Vanmarcke EH. Random fields: analysis and synthesis. Cambridge, Mass: MIT Press; 1983.
[25] Griffiths DV, Fenton GA. Bearing capacity of spatially random soil: the undrained clay Prandtl problem revisited. Geotechnique 2001;51(8):731.
[26] Fenton GA. Estimation for stochastic soil models. J Geotech Geoenviron Eng 1999;125(6):470–85.
[27] Duncan JM, Wright SG. Soil strength and slope stability. Hoboken, N.J: John Wiley & Sons; 2005.
[28] Griffiths DV, Fenton GA. Influence of soil strength spatial variability on the stability of an undrained clay slope by finite elements. In Griffiths DV, et al. editors. Slope Stability. ASCE; 2000. p. 184–93.
[29] Griffiths DV, Fenton GA. Probabilistic slope stability analysis by finite elements. J Geotech Geoenviron Eng 2004;130(5):507–18.
[30] Hicks MA, Samy K. Influence of anisotropic spatial variability on slope reliability. In Proceedings of the 8th International Symposium Numerical Models Geomech. Rome, Italy; 2002. p. 535–9.
[31] Griffiths DV, Huang JS, Fenton GA. Influence of spatial variability on slope reliability using 2-D random fields. J Geotech Geoenviron Eng 2009;135(10):1367–78.
[32] Bauer J, Pula W. Reliability with respect to settlement limit-states of shallow foundations on linearly-deformable subsoil. Comput Geotech 2000;26(3–4):281–308.
[33] Griffiths DV, Huang JS, Fenton GA. On the reliability of earth slopes in three dimensions. Proc Royal Soc A-Mathemat Phys Eng Sci 2009;465(2110):3145–64.
[34] Nadim F. Tools and strategies for dealing with uncertainty in geotechnics. In: Griffiths DV, Fenton GA, editors. Probab Methods Geotech Eng. Springer; 2007. p. 71–96.